Eur. J. Mech. B - Fluids 19 (2000) 109–122

Exact solutions for self-similar boundary-layer flows induced by permeable stretching walls

Eugen Magyari *, Bruno Keller

Physics of Buildings, Institute of Building Technology, Swiss Federal Institute of Technology (ETH) Zürich, CH-8093 Zürich, Switzerland

(Received 21 June 1999; revised 13 September 1999; accepted 14 September 1999)

Abstract – The self-similar two-dimensional steady boundary-layer flow induced by a permeable surface stretching with velocity $U_w(x) = A \cdot x^m$ in a quiescent fluid in the presence of suction or injection with velocity $V_w(x) = a \cdot x^{(m-1)/2}$ is considered for $A > 0$ and $m > -1$. The exact analytic solutions of this problem are given for $m = -1/3$ and $m = -1/2$ and the mechanical characteristics of the corresponding flows are discussed in detail. Boundary layers of the same thickness corresponding to different lateral mass fluxes are described. It is shown that to the smallest entrainment velocity, there corresponds a vanishing skin friction, i.e. a 'dragless motion' of the fluid. The exact results are also compared with the results of the analytical approximations reported recently by other authors (in a physically different but mathematically identical context) in this journal. © 2000 Éditions scientifiques et médicales Elsevier SAS

laminar boundary-layers / self-similar solutions / stretching walls / suction–injection / lateral mass flux / skin friction / entrainment

1. Introduction

Owing to their numerous applications in industrial manufacturing processes, the problems of heat and mass transfer in two-dimensional boundary layers on continuous stretching surfaces, moving in an otherwise quiescent fluid medium, have attracted considerable attention during the last few decades. Examples of such technological processes are hot rolling, wire drawing, glass-fiber and paper production, drawing of plastic films, metal and polymer extrusion and metal spinning. Both the kinematics of stretching and the simultaneous heating or cooling during such processes have a decisive influence on the quality of the final products.

Following the pioneering works of Sakiadis [1], a rapidly increasing number of papers investigating different aspects of this problem have been published. The great majority of the theoretical investigations in this field describe the heat and mass flow in the vicinity of the continuous stretching surface with the aid of similarity solutions of the two-dimensional boundary layer equations. An important feature of the corresponding boundary value problem is that it always splits into an independent flow-boundary value problem and a forced thermal convection problem. Except for exponentially stretching surfaces [2], the kinematic driving conditions of the real processes are modeled in most cases by different power-law variations of the stretching velocity $U_w(x) = A \cdot x^m$. The stretching surface is considered either as an impermeable [1–6] or as a permeable one [7–11] with a lateral mass flux of velocity $V_w(x) = a \cdot x^{(m-1)/2}$ where $a < 0$ corresponds to the suction and $a > 0$ to the injection of the fluid. As shown by Banks [4], in the range $-1 < m \leqslant -1/2$ of the stretching exponent the flow boundary value problem (and thus also the heat transfer problem) does not admit similarity solutions if the wall is impermeable ($a = 0$). More recently, in a physically different but mathematically

* Correspondence and reprints; magyari@hbt.arch.ethz.ch

identical context, Chaudhary et al. [12] have proved, however, that for $-1 \leqslant m_0(a) < m$ the similarity solutions also exist if suction ($a < 0$) is present. In this case $m_0(a) \to -1/2$ as $a \to 0$ and $m_0(a) \to -1$ as $|a| \to \infty$. The present paper shows that if $a < 0$, the similarity solution also persists for $m = -1/2$. The proof is given by deducing the corresponding exact solution (in an implicit analytic form).

The particular cases $m = 1$ and $m = -1/3$ have also attracted special attention in the past. The first case is exactly solvable for both impermeable [4, 5] and permeable [8, 9] stretching surfaces (with or without heat transfer) as well. For $m = -1/3$, the exact solution of the flow problem [4] and of the heat transfer problem [6] have been reported until now only for the impermeable case ($a = 0$). The present paper gives the solution of this flow boundary value problem also for the permeable case ($a \neq 0$) in an exact analytic form. The mechanical characteristics of the self-similar flows with $m = -1/2$ and $m = -1/3$ are then discussed in detail. Some new physical aspects of these flow problems are pointed out. Finally, we take the opportunity to compare the exact solutions (corresponding to the cases $m = 1,\ m = -1/3$, and $m = -1/2$) to analytical approximations reported recently by Chaudhary et al. in a physically different but mathematically identical context [12].

2. Basic equations

The steady velocity-boundary layer on a permeable plane wall, stretching with velocity $u_w = U_w(x)$ in a quiescent incompressible fluid of constant temperature is governed in the boundary layer approximation by equations:

$$\begin{aligned} \frac{\partial u}{\partial x} + \frac{\partial v}{\partial y} &= 0, \\ u\frac{\partial u}{\partial x} + v\frac{\partial u}{\partial y} &= \nu\frac{\partial^2 u}{\partial y^2}, \end{aligned} \tag{1}$$

accompanied by the boundary conditions:

$$u(x,0) = U_w(x), \qquad u(x,\infty) = 0, \qquad v(x,0) = V_w(x). \tag{2}$$

The x-axis is directed along the continuous stretching surface and points in the direction of motion. The y-axis is perpendicular to x and to the direction of the slot (z-axis) from where the continuous stretching plane surface issues. u and v are the x and y components of the velocity field of the steady boundary flow, respectively. ν denotes the kinamatic viscosity of the ambient fluid and will be assumed constant.

For power-law boundary conditions the present problem bears a close resemblance to the classical wedge-flow problems described by the Falkner–Skan equation (for the latter see e.g. [13−15]) with two essential differences which consist in (a) the absence of the pressure gradient term in the momentum equation and (b) in the boundary conditions (2). Nevertheless, the general functional structure of the similarity solutions is in both cases the same and is given by:

$$\begin{aligned} u(x,y) &= A\cdot x^m f'(\eta), \\ v(x,y) &= -\left(\frac{2\nu A}{m+1}\right)^{1/2}\cdot x^{(m-1)/2}\cdot\left[\frac{m+1}{2}f(\eta) + \frac{m-1}{2}\eta\cdot f'(\eta)\right], \\ \eta &= \left[(m+1)A/(2\nu)\right]^{1/2}\cdot y\cdot x^{(m-1)/2}, \end{aligned} \tag{3}$$

where the dimensionless stream function $f(\eta)$ satisfies the ordinary differential equation

$$f''' + f \cdot f'' - \frac{2m}{m+1} \cdot f'^2 = 0. \tag{4}$$

In the above equations A and m are real quantities ($A > 0,\ m > -1$) and the prime denotes a derivative with respect to the similarity variable η. The wall-boundary conditions (2) satisfied by the velocity field (3) are:

$$\begin{aligned} U_w(x) &= Ax^m \cdot f'(0), \\ V_w(x) &= -\left[\nu A(m+1)/2\right]^{1/2} \cdot x^{(m-1)/2} \cdot f(0) \equiv a \cdot x^{(m-1)/2}. \end{aligned} \tag{5}$$

The dimensionless stream function $f(\eta)$ and its first derivative are now subject to the boundary conditions:

$$f(0) = f_w, \qquad f'(0) = 1, \qquad f'(\infty) = 0, \tag{6}$$

where $f_w = -a[\nu A(m+1)/2]^{-1/2}$ will be referred to as the suction/injection parameter. Notice that $\mathrm{sgn}(f_w) = -\mathrm{sgn}(a)$. In this way $f_w = 0$ corresponds to an impermeable wall, $f_w > 0$ to suction (i.e. $V_w(x) < 0$) and $f_w < 0$ to lateral injection (i.e. $V_w(x) > 0$) of the fluid through a permeable wall.

In addition to the velocity field, the following quantities will be of interest.

- The thickness of the boundary layer δ. It is defined as the value of the y coordinate for which $u(x,\delta)/(A \cdot x^m) = f'(\eta_\delta) = 0.01$ holds. Thus the dimensional thickness δ is connected to its dimensionless counterpart η_δ by the relationship:

$$\eta_\delta = \left[(m+1)A/(2\nu)\right]^{1/2} \cdot x^{(m-1)/2} \cdot \delta. \tag{7}$$

- The entrainment velocity of the fluid:

$$v(x,\infty) = -\left[\nu A(m+1)/2\right]^{1/2} \cdot x^{(m-1)/2} \cdot f(\infty). \tag{8}$$

- The relationship between the suction/injection velocity and entrainment:

$$\frac{v(x,0)}{v(x,\infty)} = \frac{f_w}{f(\infty)}. \tag{9}$$

- The skin friction (wall shear stress) acting on the stretching surface in contact with the ambient fluid of constant density ρ:

$$\tau_w = \rho\nu \frac{\partial u}{\partial y}(x,0) = \rho\left[(m+1)\nu A^3/2\right]^{1/2} \cdot x^{(3m-1)/2} \cdot f''(0). \tag{10}$$

On the grounds of equations (8) and (10), the quantities

$$f(\infty) \equiv f_\infty \quad \text{and} \quad f''(0) \equiv f''_w \tag{11}$$

will be referred to as entrainment and skin friction parameter, respectively.

3. Exact analytic solutions for $f_w \neq 0$

3.1. The case $m = 1$

We start the discussion of the exactly solvable cases with a short review of the best known case, corresponding to linear stretching of the wall. To our knowledge, the exact solution, which in the present notation becomes:

$$f(\eta) = f_w - \frac{1}{f''_w}\left[1 - \exp\left(f''_w \cdot \eta\right)\right], \qquad f'(\eta) = \exp\left(f''_w \cdot \eta\right), \tag{12}$$

with

$$f''_w = -\frac{1}{2}\left[f_w + \left(f_w^2 + 4\right)^{1/2}\right], \tag{13}$$

was first written down by Gupta and Gupta [8].

In this case the skin friction τ_w is always negative, regardless the sign of f_w. This means that the stretching wall experiences a drag for any (finite) value of f_w. The drag only vanishes for $f_w \to -\infty$. For the impermeable wall ($f_w = 0$), one obtains $f''_w = -1$ and one recovers the solution given first by Crane [16]. The shape of the dimensionless velocity profile $f'(\eta)$ at the wall is concave for any f_w since here $f'''(0) = 1 - f_w \cdot f''_w = f''^2_w$ holds. Taking into account that

$$f_\infty = f_w - \frac{1}{f''_w} = -f''_w, \tag{14}$$

the entrainment velocity becomes $v(x, \infty) = (\nu A)^{1/2} \cdot f''_w$.

The dimensionless thickness η_δ of the boundary layer is now given by the explicit expression:

$$\eta_\delta = \left[\left(f_w^2 + 4\right)^{1/2} - f_w\right] \cdot \ln 10. \tag{15}$$

Hence, one may conclude that, as the parameter f_w varies from negative (injection) to positive (suction) values, the entrainment parameter f_∞ increases, while the thickness of the boundary layer decreases monotonically, according to the exact equations (13), (14) and (15). Except for the downstream velocity $u(x, y)$, all other physical quantities are now independent of the wall coordinate x.

3.2. The case $m = -1/3$

After two successive integrations, equation (4) together with the boundary conditions (6) lead in this case to the separable (Riccati-type) equation:

$$f' + \frac{1}{2}f^2 = 1 + \frac{1}{2}f_w^2, \tag{16}$$

and to the relationships

$$f''_w = -f_w \quad \text{and} \quad f_\infty = \left(f_w^2 + 2\right)^{1/2}. \tag{17}$$

Thus, the boundary value problem (4) and (6) admits an elementary solution again. It is:

$$f(\eta) = f_\infty \cdot \frac{f_\infty \cdot \sinh(f_\infty \cdot \eta/2) + f_w \cdot \cosh(f_\infty \cdot \eta/2)}{f_w \cdot \sinh(f_\infty \cdot \eta/2) + f_\infty \cdot \cosh(f_\infty \cdot \eta/2)}. \tag{18}$$

The dimensionless downstream velocity is given by:

$$f'(\eta) = f_\infty^2 \cdot \left[f_w \cdot \sinh(f_\infty \cdot \eta/2) + f_\infty \cdot \cosh(f_\infty \cdot \eta/2) \right]^{-2}. \tag{19}$$

Therefore, the stretching surface experiences in this case a negative skin friction (i.e. a viscous drag) for $f_w > 0$ (suction), and a positive one (i.e. a viscous driving force) for $f_w < 0$ (injection). In the impermeable case ($f_w = 0$) no viscous shear acts between the stretching surface and the induced motion of the fluid. The entrainment parameter f_∞ reaches here its smallest value, $(f_\infty)_{\min} = 2^{1/2}$. Concerning the shape of the dimensionless velocity profile $f'(\eta)$ at the wall, equations (4) and (17) imply $f'''(0) = f_w^2 - 1$. Therefore, as f_w decreases from $+\infty$ to $-\infty$, the shape of $f'(\eta)$ at the wall changes from concave to convex as the value $f_w = 1$ is reached. For $1 > f_w > -1$ the shape at the wall is still convex and for $f_w < -1$ becomes concave again (*figure 1*). As one switches from suction ($f_w > 0$) to injection ($f_w < 0$), which implies a change from negative to positive skin friction, in the velocity profiles a maximum may be observed. This maximum

$$f'_* = 1 + \frac{1}{2} f_w^2, \tag{20}$$

is located at

$$\eta^* = \frac{1}{f_\infty} \cdot \ln\left(1 + |f_w| \cdot f_\infty + f_w^2\right). \tag{21}$$

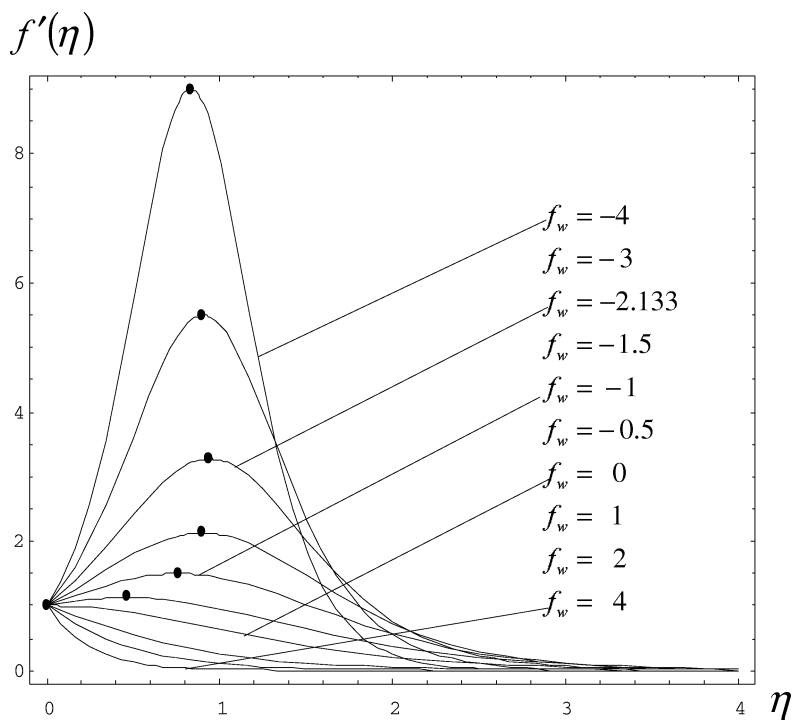

Figure 1. Profiles of the dimensionless downstream velocity $f'(\eta)$ for $m = -1/3$ as plotted against η for different values of the suction/injection parameter f_w. The dots indicate the velocity maxima occurring for $f_w < 0$. Their coordinates (η_*, f'_*) are given by equations (21) and (20). The largest value of η^* is reached for $f_w = -2.133$ and amounts to $\eta^*_{\max} = 0.937$.

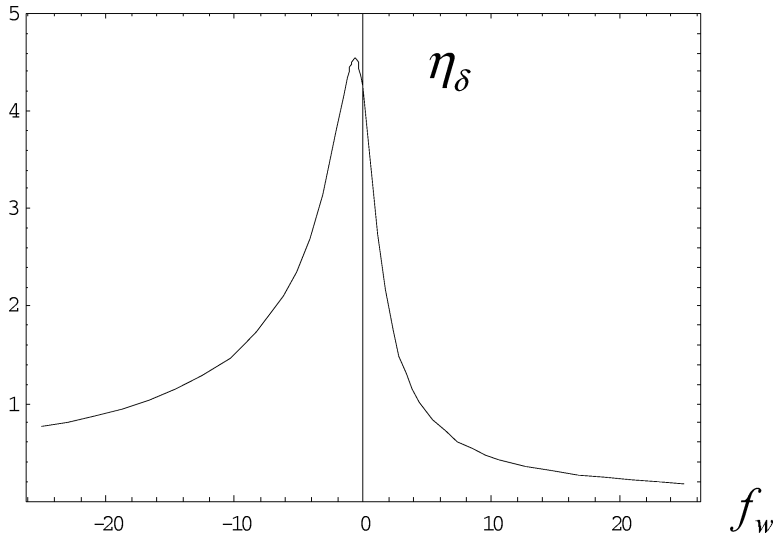

Figure 2. The dimensionless thickness η_δ of the boundary layer for $m=-1/3$ as plotted against the suction/injection parameter f_w. The maximum $\eta_{\delta,\max}=4.542$ is reached for $f_w=-0.617$.

One immediately sees that for $f_w\to-\infty$, $f'_*\to+\infty$ as $f_w^2/2$, while η^* goes slowly to zero as $2(\ln|f_w|)/|f_w|$, i.e. f'_* returns to its initial location $\eta^*=0$ corresponding to $f_w=0$. The largest value of η^* is reached for $f_w=-2.133$ and is equal to $\eta^*_{\max}=0.937$, *figure 1*.

The dimensionless thickness η_δ of the boundary layer is given again by an explicit formula:

$$\eta_\delta=\frac{2}{f_\infty}\cdot\ln\left[\frac{10\cdot f_\infty+(100f_\infty^2-2)^{1/2}}{f_w+f_\infty}\right]. \tag{22}$$

The thickness of the boundary layer goes in this case to zero for both $f_w\to\pm\infty$ and reaches a maximum in between, $(\eta_\delta)_{\max}=4.542$ for $f_w=-0.617$. This behavior is illustrated in *figure 2*, which also shows the existence of two boundary-layers of the same thickness $\eta_\delta<(\eta_\delta)_{\max}$ which correspond to two different values $f_{w1,2}$ of the suction/injection parameter so that $f_{w1}<-0.617<f_{w2}$. As an illustration, in *figure 3* the dimensionless velocity profiles of two boundary layers of thickness $\eta_\delta=4$, corresponding to $f_{w1}=-2.513$ and $f_{w2}=0.577$ are shown.

It is worthwhile to mention that for $f_w=0$ in equations (18) one immediately recovers the well known Schlichting–Bickley-type free-jet solution $f(\eta)=2^{1/2}\cdot\tanh(\eta/2^{1/2})$ as reported in [4] and [6].

3.3. The case $m=-1/2$

We start the investigation of the case $m=-1/2$ with the integral equation:

$$2f\cdot f''+2f^2\cdot f'-f'^2+\frac{4(2m+1)}{m+1}\cdot\int_\eta^\infty f\cdot f'^2(\eta)\,d\eta=0, \tag{23}$$

which is obtained by integration of equation (4) after multiplication by $f(\eta)$, by taking into account that $f'(\infty)=0$ and by assuming that $f''(\infty)=0$. By substituting $\eta=0$ in (23), one immediately recovers the result of Banks [4] which states that along the impermeable ($f_w=0$) stretching wall no similar boundary flow

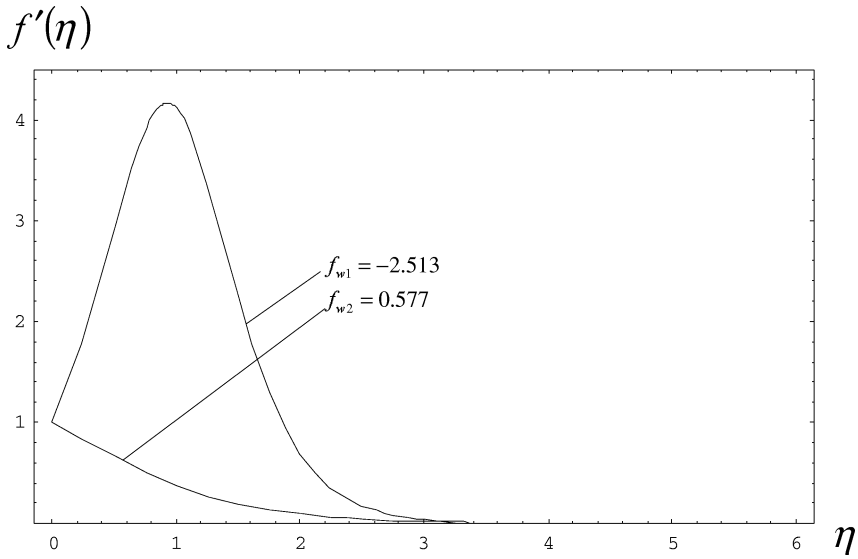

Figure 3. Dimensionless downstream velocity profiles of the boundary layers of thickness $\eta_\delta = 4$, corresponding (in the case $m = -1/3$) to $f_{w1} = -2.513$ and $f_{w2} = 0.577$, respectively.

satisfying the boundary conditions (6) exists if $-1 \leqslant m \leqslant -1/2$. One sees however that, if a lateral mass flux is present ($f_w \neq 0$), the existence of such a boundary layer for $-1 < m \leqslant -1/2$, may no longer be excluded on the grounds of equation (23). In particular, for $m = -1/2$ equation (23) reduces to:

$$2f \cdot f'' + 2f^2 \cdot f' - f'^2 = 0. \tag{24}$$

Thus, with the aid of the boundary conditions (6) one immediately obtains:

$$f''_w = \frac{1 - 2f_w^2}{2f_w}. \tag{25}$$

As it will be shown below, only positive values of f_w are allowed in equation (25). For this reason, the boundary layer cotarresponding to the parameter values $m = -1/2$ and $f_w > 0$, will be referred to hereafter as being a 'suction-generated' flow. From equations (4), (6) and (25) one obtains for the curvature of the dimensionless velocity profile $f'(\eta)$ at the wall: $f'''(0) = f_w^2 - 5/2$.

In order to obtain the solution which describes the suction-generated boundary layer, one has now to solve instead of (4), the second order equation (24) with the boundary conditions (6). Fortunately, equation (24) admits an integrating factor so that it may be transcribed in the form

$$f^{-3/2} \cdot (2f \cdot f'' + 2f^2 \cdot f' - f'^2) = 2(f^{-1/2} \cdot f' + 2f^{3/2}/3)' = 0.$$

Thus, $f^{-1/2} \cdot f' + 2f^{3/2}/3 =$ constant and, by taking into account the boundary conditions (6), one gets:

$$f' = \frac{2}{3} f_\infty^2 (W - W^4), \tag{26}$$

where

$$W = W(\eta) = \left[\frac{f(\eta)}{f_\infty}\right]^{1/2} \tag{27}$$

and

$$f_\infty = 2^{-2/3} \cdot f_w^{-1/3} \cdot \left(2f_w^2 + 3\right)^{2/3}. \tag{28}$$

Hence, equation (26) determines the dimensionless velocity profile f' as an explicit function of the dimensionless stream function f and the suction parameter f_w. The functional dependences $f = f(\eta)$ and $W = W(\eta)$ should then result by further integration of (26). After some calculus one obtains that $W = W(\eta)$ satisfies the transcendental equation

$$\eta = \frac{1}{f_\infty} \cdot \ln\left[\frac{F(W_0)}{F(W)}\right], \tag{29}$$

where

$$F(W) = (1 - W)\left(1 + W + W^2\right)^{-1/2} \cdot \exp\left[-3^{1/2} \cdot \arctan\left(\frac{1 + 2W}{3^{1/2}}\right)\right] \tag{30}$$

and

$$W_0 = \left(\frac{f_w}{f_\infty}\right)^{1/2} = \left(\frac{2f_w^2}{2f_w^2 + 3}\right)^{1/3}. \tag{31}$$

For $\eta \to \infty$, according to (27) and (30) one has $W \to 1$ and $F(W) \to 0$, which, according to (29) requires $f_\infty > 0$. Thus, equation (28) requires $f_w > 0$, as anticipated above.

The transcendental equation (29) can be inverted to $W = W(\eta)$ numerically as well as analytically (for the analytical procedure see the Appendix). By performing this operation, the velocity profile $f'(\eta)$ results then from (26) for any given $f_w > 0$ explicitly. The curves of *figure 4* have been obtained by plotting the implicit function (29). The main characteristics of the velocity profiles shown in *figure 4* can be easily extracted from the above equations. First of all, equations (25) and $f'''(0) = f_w^2 - 5/2$ show that by switching on a massive suction ($f_w \gg 1$) the skin friction parameter f_w'', i.e. the slope at the wall of the main velocity profile of the induced downstream flow is negative and its shape is concave, $f'''(0) > 0$. The skin friction is also negative, i.e. the stretching wall experiences a (considerable) drag. This situation persists down to the value $f_w = 2^{-1/2}$, except for the fact that for $0 < f_w < (5/2)^{1/2}$ the shape of the velocity profile at the wall has changed from concave to convex, by passing through $f_w = (5/2)^{1/2}$ which is a shape with vanishing curvature. As $f_w = 2^{-1/2}$ is reached, the skin friction becomes zero, i.e. the drag vanishes. The entrainment parameter reaches here its minimum value, $(f_\infty)_{\min} = 2^{5/6}$. Below the threshold value $f_w = 2^{-1/2}$ corresponding to the zero-drag profile (where the shape at the wall still remains convex), the slope f_w'' of the velocity profile and thus also the skin friction, become positive. Hence, the steady wall experiences a viscous driving force for $0 < f_w < 2^{-1/2}$. In the parameter range $0 < f_w < 2^{-1/2}$ the change to a positive skin friction is accompanied by the occurrence of a maximum in the profile of the downstream velocity $f'(\eta)$. As f_w decreases from $2^{-1/2}$ to zero, the maximum $f'_{\max} = f'(\eta^*)$ increases from 1 to infinity according to

$$f'_{\max} = 2^{-5/3} \cdot f_\infty^2 = 2^{-3} \cdot f_w^{-2/3} \cdot \left(2f_w^2 + 3\right)^{4/3}, \tag{32}$$

while its locus $\eta = \eta^*$ returns to $\eta^* = 0$ according to

$$\eta^* = \frac{1}{f_\infty} \ln\left[\frac{F(W_0)}{F(2^{-2/3})}\right], \tag{33}$$

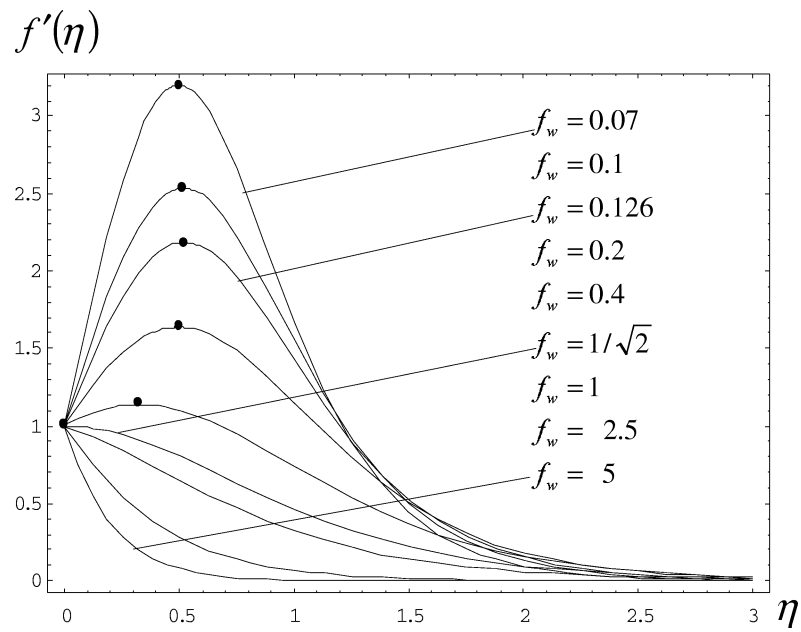

Figure 4. Profiles of the dimensionless downstream velocity $f'(\eta)$ for $m = -1/2$ as plotted against η for different values of the suction parameter $f_w > 0$. The dots indicate the velocity maxima occurring for $0 < f_w < 2^{-1/2}$. Their coordinates (η_*, f'_*) are given by equations (33) and (32). The largest value of η^* is reached for $f_w = 0.126$ and amounts to $\eta^*_{\max} = 0.521$.

by reaching for $f_w = 0.126027$ the maximum deviation $\eta^*_{\max} = 0.520646$ from the f' axis. This dependence of η^* on f_w is also shown in *figure 4*.

The dimensionless thickness η_δ of the boundary layer is now given by:

$$\eta_\delta = \frac{1}{f_\infty} \cdot \ln\left[\frac{F(W_0)}{F(W_\delta)}\right], \tag{34}$$

where, according to (26),

$$W_\delta^4 - W_\delta + 0.015 \cdot f_w^{-2} = 0. \tag{35}$$

This equation has for any $f_w > 0$ two complex and two real and positive roots. Taking into account that the smallest value of f_∞ (which is reached for $f_w = 2^{-1/2}$) amounts to $2^{5/6} \cong 1.78$, the largest value of the free term $\varepsilon = 0.015 \cdot f_\infty^{-2}$ in (35) is $4.72 \cdot 10^{-3}$. Thus, the real roots of (35) can be approximated to high accuracy by $W_{\delta 1} = 1 - \varepsilon/3$ and $W_{\delta 2} = \varepsilon$. In the present context, the physical solution is the first one, i.e.:

$$W_\delta = 1 - 0.005 \cdot f_\infty^{-2}. \tag{36}$$

In this way, one immediately obtains for η_δ the approximation:

$$\eta_\delta = \frac{1}{f(\infty)} \cdot \ln\left[200 \cdot 3^{1/2} f_\infty^2 \cdot F(W_0) \exp\left(\pi \cdot 3^{-1/2}\right)\right]. \tag{37}$$

Table I illustrates the performance of the approximation formula (36) compared to the corresponding numerical solution of equation (35), as well as the performance of (37) and (A.10) compared to the exact result (34) for η_δ. As f_w decreases from $+\infty$ to 0, the thickness of the boundary layer increases from zero to the

Table I. Exact and approximate values of W_δ and η_δ for different values of f_w.

f_w	W_δ		η_δ		
	Equation (35); 'Exact'	Equation (36); Approximate	Equations (34), (35); 'Exact'	Equation (37); Approximate	Equation (A.10); Approximate
0.1	0.999377	0.999378	2.917464	2.918123	2.917463
0.5	0.998502	0.998506	3.459076	3.461534	3.459068
1	0.998522	0.998526	2.969126	2.971534	2.969118
2.5	0.999399	0.999399	1.668995	1.669620	1.668994
5	0.999815	0.999815	0.897008	0.897115	0.897008

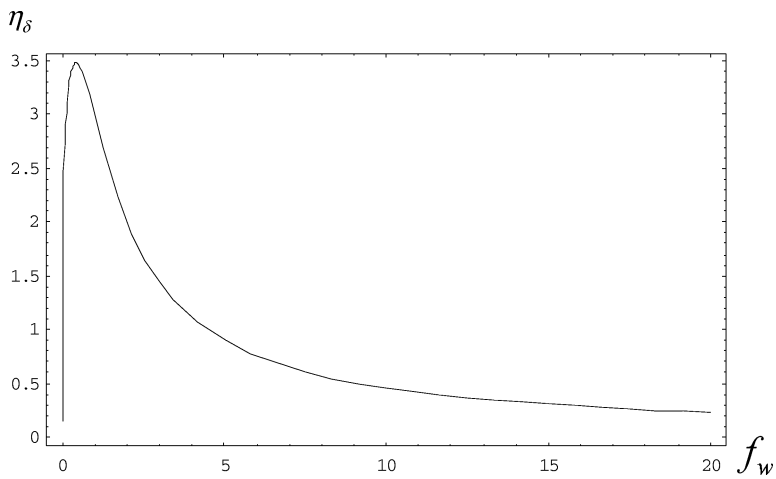

Figure 5. The dimensionless thickness η_δ of the boundary layer for $m = -1/2$ as plotted against the suction parameter $f_w > 0$. The maximum $\eta_{\delta,\max} = 3.485$ is reached for $f_w = 0.407$.

maximum value $(\eta_\delta)_{\max} = 3.484820$ which is attained for $f_w = 0.406634$ and then decreases, approaching zero as $f_w \to 0$. This behavior is illustrated in *figure 5*, which shows again the existence of boundary-layers of the same thickness $\eta_\delta < (\eta_\delta)_{\max}$ corresponding to two different values $f_{w1,2}$ of the suction parameter so that $0 < f_{w1} < 0.406634 < f_{w2}$.

4. Comparison with earlier analytical approximations

The aim of the present section is to compare the exact analytic solutions corresponding to the stretching exponents $m = 1$, $m = -1/3$ and $m = -1/2$ with the results of the analytical approximations reported recently by Chaudhary et al. [12] in connection with the boundary-layer flows adjacent to vertical permeable surfaces in saturated porous media.

The physical problem investigated in [12] reduces to the two-point boundary value problem:

$$\widetilde{f}''' + (\widetilde{m} + 1)\,\widetilde{f} \cdot \widetilde{f}'' - 2\widetilde{m} \cdot \widetilde{f}'^2 = 0, \tag{38a}$$

$$\widetilde{f}(0) = -\gamma, \qquad \widetilde{f}'(0) = 1, \qquad \widetilde{f}'(\infty) = 0, \tag{38b}$$

where to the dimensionless stream function f, the similarity variable η and to the power-law exponent m of reference [12] a 'tilde' has now been added.

In spite of their different physical origin, the boundary value problems, (4) and (6) and (38a), (38b), are mathematically equivalent. Indeed, it is easy to show that these problems may be mapped to each other by the simple scaling relationships:

$$\begin{aligned} &m = \widetilde{m}, \qquad \eta = (1+m)^{1/2}\cdot\widetilde{\eta}, \qquad f(\eta) = (1+m)^{1/2}\cdot\widetilde{f}(\widetilde{\eta}), \\ &f_w = -(1+m)^{1/2}\cdot\gamma \quad \text{and} \quad f''(0) = (1+m)^{-1/2}\cdot\widetilde{f}''(0). \end{aligned} \tag{39}$$

In this way, for $m = 1$ the exact solution of the boundary value problem (38a), (38b), as obtained from (12), (13) and (39) reads:

$$\widetilde{f}(\widetilde{\eta}) = -\gamma - \frac{1}{\widetilde{f}''(0)}\left[1 - \exp\left(\widetilde{f}''(0)\cdot\widetilde{0}\right)\right], \tag{40}$$

$$\widetilde{f}'(\widetilde{\eta}) = \exp\left(\widetilde{f}''(0)\cdot\widetilde{\eta}\right), \tag{41}$$

with

$$\widetilde{f}''(0) = \gamma - \left(\gamma^2 + 2\right) = -\widetilde{f}_\infty. \tag{42}$$

The family of curves obtained by numerical integration of (38a), (38b) and shown in figure 4b of reference [12] is just the plot of the exact solution (41), (42) for $\gamma = 0,\ 4,\ 8$ and 12.

In figure 7b of reference [12], also obtained by numerical integration of (38a), (38b), one immediately recovers $-\widetilde{f}''$ as plotted against γ according to (42).

The quantities:

$$\widetilde{f}''(0) = \frac{2}{3}\gamma, \quad \widetilde{f}_\infty = \left(\gamma^2 + 3\right)^{1/2} \quad \text{valid for } m = -1/3, \tag{43}$$

$$\widetilde{f}''(0) = \frac{\gamma^2 - 1}{2\gamma}, \quad \widetilde{f}_\infty = \gamma^{-1/3}\cdot\left(\gamma^2 + 3\right)^{2/3} \quad \text{valid for } m = -1/2, \tag{44}$$

may be compared with reference [12] for $\gamma = -1$ only. The corresponding points can be recovered in figures 3a and 3b of reference [12] with a good precision.

For the case of massive suction ($\gamma < 0,\ |\gamma| \to \infty$) and any $m > -1$, according equation (29c) of reference [12], holds:

$$\widetilde{f}''(0) = -|\gamma|(1+m)\left[1 + \frac{3m+1}{2(1+m)^2\cdot\gamma^2} + \cdots\right].$$

It is now easy to see that for $m = 1$ this approximation formula is just the series expansion of $\widetilde{f}''$ given by (42). The salient feature of the approximation formula ([12], 29c) is that for $m = -1/3$ it reproduces the exact result (43) to leading order in γ, whereas for $m = -1/2$ it yields the exact result (44) by its first two terms. This means that for $m = -1/3$, in equation (29c) of reference [12] the entire square bracket, except for its first term, and for $m = -1/2$ all its terms beyond the first two, should supply an identically vanishing contribution.

Similarly to ([12], 29c), the approximation formula ([12], 35):

$$\widetilde{f}''(0) = -\frac{1-\alpha}{\gamma}\left[1 - \frac{(1+\alpha)(1-2\alpha)}{2\gamma^2} + \cdots\right]$$

which should hold for the case of a massive injection, $\gamma \to \infty$ and for any $\alpha = (1-m)/(1+m)$ and $m > -1/2$, represents for $m = 1$ (i.e. $\alpha = 0$) the series expansion of the exact result given by (42). For $m = -1/3$, however, ([12], 35) deviates from the exact result (43) substantially.

Finally, it is worthwhile to mention that the limiting case $m \to \infty$ of the power-law models corresponds to the case of the boundary-layer flows induced by exponentially stretching surfaces [2, 4]. Thus, in the approximation formula ([12], 39) one immediately recovers the skin friction parameter -1.281808 of the exponential stretching [2, 4] to excellent accuracy.

5. Summary and conclusions

In the present paper, the two-dimensional boundary-layer flows induced by permeable stretching surfaces have been considered. The exact analytic solutions corresponding to the stretching exponents $m = 1$, $m = -1/3$ and $m = -1/2$ have been derived. The mechanical characteristics of these boundary layers, described by their (dimensionless) thickness η_δ, skin friction parameter f''_w and entrainment parameter f_∞ (as functions of the suction/injection parameter f_w) have been examined in detail. The main physical results of the paper may be summarized as follows.

1. For $m = 1$, as f_w varies from negative (injection) to positive (suction) values, the entrainment parameter f_∞ increases, while the thickness of the boundary layer decreases monotonically. The skin friction τ_w is always negative, regardless the sign of f_w. This means that the stretching wall experiences a viscous drag for any finite f_w.
2. For $m = -1/3$, the stretching surface experiences a negative skin friction (i.e. a viscous drag) for $f_w > 0$ (suction), and a positive one (i.e. a viscous driving force) for $f_w < 0$ (injection). In the impermeable case ($f_w = 0$) no viscous shear acts between the stretching surface and the induced motion of the (no slip) fluid. Simultaneously with the change from negative to positive skin friction, in the profiles of the downstream velocity a maximum occurs (*figure 1*). The trajectory described by this maximum as f_w varies from 0 to $-\infty$ is marked in *figure 1* by dots. During the variation of f_w from $+\infty$ to $-\infty$, the thickness of the boundary layer increases from zero to a maximum value $(\eta_\delta)_{\max} = 4.542$ which is reached for $f_w = -0.616$ and goes then to zero again. This behavior is illustrated in *figure 2*, which also shows the existence of two boundary-layers of the same thickness $\eta_\delta < (\eta_\delta)_{\max}$ corresponding to two different values of the suction/injection parameter f_w (see also *figure 3*).
   It is worthwhile to mention here that the dragless motion does not mean that for $\tau_w = 0$ the fluid separates from the stretching wall, since in the case of the boundary layers on moving surfaces equation $\tau_w(x) = 0$ is not sufficient for the determination of the separation point. Instead, the so called MRS-criterion (Moore–Rott–Sears-criterion) applies here (see reference [14, p. 317]). According to the MRS-criterion, the separation occurs in that point of the boundary layer where (in the present notations) both equations $f'(\eta) = f''(\eta) = 0$ are satisfied. Obviously, in the cases discussed here, no $\eta < \infty$ satisfying both of these equations exists.
3. The case $m = -1/2$ shows a qualitative resemblance with the case $m = -1/3$ (compare *figures 1* and *2* to *figures 4* and *5*, respectively), with the essential difference that this similarity flow only exists if suction ($f_w > 0$) is present and it disappears as the suction is switched off. The dragless motion ($\tau_w = 0$) corresponds in this case to the value $f_w = 2^{-1/2}$ of the suction parameter. The exact solution is obtained for $m = -1/2$ in the implicit form (29), which (as shown in the Appendix) may be inverted by a Lagrange-expansion to an explicit form.
4. All the exact solutions presented above show for $\eta \to \infty$ an exponential decay of the form:

$$f(\eta) \to f_\infty - \frac{B}{f_\infty} e^{-f_\infty \cdot \eta},$$

   where B is a function of f_w (for $m = 1$, $B = 1$).

Table II. The zero $f_w = f_w^0$ of the skin friction parameter f_w'' minimizes the entrainment parameter f_∞.

m	f_w^0	f_∞	$(f_\infty)_{\min}$
1	$-\infty$	$\frac{1}{2}[f_w + (f_w^2+4)^{1/2}]$	0
$-1/3$	0	$(f_w^2+2)^{1/2}$	$2^{1/2}$
$-1/2$	$2^{-1/2}$	$2^{-2/3} f_w^{-1/3}(2f_w^2+3)^{2/3}$	$2^{5/6}$

5. A further remarkable feature of the boundary-layer flows discussed is that the value f_w^0 of the suction/injection parameter f_w for which the skin friction parameter f_w'' vanishes, minimizes the entrainment parameter f_∞. In other words, the dragless motion of the fluid always corresponds to the smallest possible entrainment. This circumstance (which is presumably valid for any $-1 < m \leqslant 1$) is summarized for $m = 1,\ m = -1/3$ and $m = -1/2$ in *table II*.
6. The exact solutions for $m = 1,\ m = -1/3$ and $m = -1/2$ also reveal some interesting features of the analytical approximations of other authors, reported recently in connection with the boundary-layer flows in saturated porous media [12].

Appendix

The analytical inversion of the transcendental equation (29) to $W = W(\eta)$ can be accomplished as follows. If

$$y = a + b \cdot G(y), \tag{A.1}$$

where G is a function of y which is analytic for $y = a$, and a and b are independent of y, the solution of this implicit equation is given by the Lagrange expansion [17]:

$$y = a + \sum_{n=1}^{\infty} \left[\frac{d^{n-1}}{dz^{n-1}} G^n(z) \right]_{z=a} \cdot \frac{b^n}{n!}. \tag{A.2}$$

The Lagrange-expansion of an arbitrary function $\Phi = \Phi(y)$ of this y reads then [17]:

$$\Phi(y) = \Phi(a) + \sum_{n=1}^{\infty} \left\{ \frac{d^{n-1}}{dz^{n-1}} \left[G^n(z) \cdot \frac{d\Phi(z)}{dz} \right] \right\}_{z=a} \cdot \frac{b^n}{n!}. \tag{A.3}$$

Our equation (29) may be put in the form (A.1) with $y = W,\ a = 1$,

$$b = \exp(-f_\infty \cdot \eta), \tag{A.4}$$

and

$$G(W) = -F(W_0) \cdot \left(1 + W + W^2\right)^{1/2} \exp\left[3^{1/2} \cdot \arctan\left(\frac{1+2W}{3^{1/2}} \right) \right]. \tag{A.5}$$

Thus, the Lagrange-expansions of $W = W(\eta)$ and $f' = f'(\eta)$ are:

$$W(\eta) = 1 + \sum_{n=1}^{\infty} \left(\left[\frac{d^{n-1}}{dz^{n-1}} G^n(z) \right]_{z=1} \frac{e^{-n \cdot f_\infty \cdot \eta}}{n!} \right), \tag{A.6}$$

$$f'(\eta) = \frac{2f_\infty^2}{3} \cdot \sum_{n=1}^{\infty} \left(\left[\frac{d^{n-1}}{dz^{n-1}} \left[(1-4z^3) G^n(z) \right] \right\}_{z=1} \frac{e^{-n \cdot f_\infty \cdot \eta}}{n!} \right). \tag{A.7}$$

For $\eta \gg 1$, these expansions converge rapidly. In the approximation of first order we obtain:

$$f'(\eta) \cong 2 \cdot 3^{1/2} \cdot f_\infty^2 \cdot F(W_0) \cdot \exp\left(\frac{\pi}{3^{1/2}} - f_\infty \cdot \eta \right). \tag{A.8}$$

According to the definition $f'(\eta_\delta) = 0.01$, we get thus for the dimensionless thickness of the boundary layer, in the approximation of first order:

$$\eta_\delta \equiv \eta_{\delta 1} = \frac{1}{f_\infty} \cdot \ln\left[200 \cdot 3^{1/2} f_\infty^2 \cdot F(W_0) \exp\left(\pi \cdot 3^{-1/2} \right) \right], \tag{A.9}$$

which coincides exactly with the expression (37) obtained by algebraic approximation. The second order approximation of (A.7) yields for η_δ the expression:

$$\eta_{\delta 2} = \eta_{\delta 1} + \frac{1}{f_\infty} \ln\left[1 + \left(1 - \frac{3}{50 \cdot f_\infty^2} \right)^{1/2} \right] - \frac{\ln 2}{f_\infty}. \tag{A.10}$$

The performance of (A.10) compared to (A.9) and to the exact result (34) is shown in *table I.*

References

[1] Sakiadis B.C., Boundary-layer behavior on continuous solid surfaces, AIChE J. 7 (1961) 26–28; 221–225; 467–472.
[2] Magyari E., Keller B., Heat and mass transfer in the boundary layers on an exponentially stretching continuous surface, J. Phys. D Appl. Phys. 32 (1999) 577–585.
[3] Ali M.E., Heat transfer characteristics of a continuous stretching surface, Wärme Stoffübertrag. 29 (1994) 227–234.
[4] Banks W.H.H., Similarity solutions of the boundary layer equations for a stretching wall, J. Mécanique Theorique Appliquée 2 (1983) 375–392.
[5] Grubka L.J., Bobba K.M., Heat transfer characteristics of a continuous stretching surface with variable temperature, J. Heat Trans-T ASME 107 (1985) 248–250.
[6] Magyari E., Keller B., Heat transfer characteristics of the separation boundary flow induced by a continuous stretching surface, J. Phys. D Appl. Phys. 32 (1999) 2876–2881.
[7] Erickson L.E., Fan L.T., Fox V.G., Heat and mass transfer on a moving continuous flat plate with suction or injection, Ind. Eng. Chem. Res. 5 (1966) 19–25.
[8] Gupta P.S., Gupta A.S., Heat and mass transfer on a stretching sheet with suction or blowing, Can. J. Chem. Eng. 55 (1977) 744–746.
[9] Chen C.K. and Char M.I., Heat transfer of a continuous stretching surface with suction or blowing, J. Math. Anal. Appl. 135 (1988) 568–580.
[10] Ali M.E., On thermal boundary layer on a power-law stretched surface with suction or injection, Int. J. Heat Mass Trans. 16 (1995) 280–290.
[11] Elbashbeshy E.M.A., Heat transfer over a stretching surface with variable surface heat flux, J. Phys. D Appl. Phys. 31 (1998) 1951–1954.
[12] Chaudhary M.A., Merkin J.H., Pop I., Similarity solutions in the free convection boundary-layer flows adjacent to vertical permeable surfaces in porous media. I. Prescribed surface temperature, Eur. J. Mech. B-Fluid. 14 (1995) 217–237.
[13] Eckert E.R.G., Drake R.M., Analysis of Heat and Mass Transfer, McGraw-Hill, New York, 1972.
[14] Schlichting H., Gersten K., Grenzschicht-Theory, Springer-Verlag, Berlin, 1997.
[15] Bejan A., Convection Heat Transfer (2nd ed.), John Wiley & Sons, New York, 1995.
[16] Crane L.E., Flow past a stretching plane, Z. Angew. Math. Phys. 21 (1970) 645–647.
[17] Whittaker E.T., Watson G.N., A Course of Modern Analysis, Cambridge Univ. Press, London, 1927, pp. 132–133.